

Microstructure and Texture Evolution in a Magnesium Alloy During Processing by High-Pressure Torsion

Yi Huang^{a*}, Roberto B. Figueiredo^b, Thierry Baudin^c, Anne-Laure Helbert^c,

François Brisset^c, Terence G. Langdon^{a,d}

^aMaterials Research Group, Faculty of Engineering and the Environment,
University of Southampton, Southampton SO17 1BJ, U.K.

^bDepartment of Materials Engineering and Civil Construction, Universidade Federal de Minas Gerais – UFMG,
CEP 31270-901, Belo Horizonte, MG, Brazil

^cICMMO, UMR CNRS 8182 - Bât 410, Université Paris-Sud, 91405 Orsay Cedex, France

^dDepartments of Aerospace & Mechanical Engineering and Materials Science,
University of Southern California, Los Angeles, CA 90089-1453, U.S.A.

Received: September 6, 2012; Revised: October 25, 2012

Magnesium alloys often exhibit cracking and segmentation after equal-channel angular pressing (ECAP) at room temperature. With torsion shear deformation and a hydrostatic stress, high-pressure torsion (HPT) has an advantage over ECAP in the processing of hard-to-deform materials like magnesium alloys at room temperature. In this report, HPT was used on extruded AZ31 Mg alloy at temperatures of 296, 373 and 473 K for 1 and 5 turns. After HPT processing, the hcp crystal c-axis rotated from the disc (r, θ) plane towards the torsion axis. The angle between the c-axis and the torsion axis (ϕ) has a relationship with the HPT processing temperature. It was found that the c-axis was 10° from the torsion axis at 296 and 373 K but 5° from the torsion axis at 473 K. The activity of the basal $\langle a \rangle$ slip and the twinning exert significant contributions to the deformation. Microstructural features such as the grain size and grain size distributions were examined and correlated with the mechanical properties through the microhardness values.

Keywords: *high-pressure torsion, magnesium alloys, microstructure, texture*

1. Introduction

Severe plastic deformation (SPD) has been widely used for producing bulk metallic materials that have ultra-fine grain size and enhanced strength¹. Equal-channel angular pressing (ECAP)² and high-pressure torsion (HPT)³ are the most popular and feasible techniques for SPD. Soft materials like Cu and Al alloys can be processed by ECAP at room temperature^{4,7}. However, hard materials such as magnesium alloys are generally processed at high temperatures (423-523 K) by ECAP due to their poor ductility at lower temperatures⁸⁻¹⁰. Magnesium alloys often exhibit cracking and segmentation after ECAP at room temperature¹¹⁻¹⁴ so that the processing temperature is important in limiting the grain refinement and strength improvement of magnesium alloys. With torsion shear deformation and a hydrostatic stress, HPT has an advantage over ECAP in the processing of hard-to-deform materials like magnesium alloys at room temperature. Thus, it is expected that room temperature HPT processing will prevent segmentation and cracking due to the large hydrostatic pressure imposed in HPT.

There are some recent results on the HPT processing of the magnesium AZ31 at temperatures of 453 K^[15] and 463 K^[16,17] but so far there are only limited reports on the

processing of this alloy at room temperature^{18,19}. An inherent problem in the processing of magnesium alloys by SPD is the hcp crystal structure which limits the numbers of active slip systems and leads to a difficulty in forming structural components. A study of the activity of the slip system and twinning contribution at different temperatures in HPT will be useful in understanding the deformation mechanism. It is necessary also to study the texture introduced into the AZ31 alloy as a function of different HPT processing temperatures. The present investigation was designed to determine the evolution of microstructures and textures in an AZ31 alloy processed by HPT at temperatures from 296 to 473 K.

2. Experimental Material and Procedures

The material used in this study was a commercial AZ31 alloy (Mg-3% Al-1% Zn) supplied in the form of extruded rods having a diameter of 10 mm. The material was obtained from Timminco Corporation (now Applied Magnesium International), Aurora, CO. The as-received material had an average grain size $\sim 10 \mu\text{m}$ and a Vickers microhardness, Hv, ~ 55 ^[15]. The extruded rods were sliced into discs with thicknesses of ~ 1.2 mm and then ground with abrasive papers to final thicknesses of ~ 0.8 mm.

*e-mail: y.huang@soton.ac.uk

The discs were processed by HPT under quasi-constrained conditions³ through total numbers of turns, N , of 1 or 5 at temperatures of 296, 373 or 473 K using an imposed pressure of 6.0 GPa and a rotational speed for the lower anvil of 1 rpm. A small furnace was placed around the upper and lower anvils for heating and the temperature was controlled to within ± 5 K using a thermocouple placed within the upper anvil²⁰.

After HPT processing, the discs were mounted, ground and polished, then etched using an acetic picric solution (5 mL of acetic acid, 6 g of picric acid, 10 mL of water and 100 mL of ethanol). The microstructures were examined using an Olympus optical microscope (OM) and a FEI Quanta 250 FEG scanning electron microscope (SEM). Representative images of the grain structures were recorded at different locations along the diameter of each disc at the centre, half-radius and the edge positions. Using these OM and SEM micrographs, grain sizes were measured using the linear intercept method with a count of at least 400 grains. Measurements were taken along a number of different lines and then the average grain sizes and the associated 95% error bars were estimated.

The Vickers microhardness, H_v , was measured on polished mirror-like disc surfaces using a Zwick Indentec microhardness tester equipped with a Vickers indenter. The hardness measurements used a load of 200 gf and dwell times of 10 s. These measurements were taken at positions along the disc diameter separated by incremental distances of 0.3 mm with four individual points recorded around each selected position separated from this position by distances of 0.15 mm. These measurements were used to provide the variations of hardness across each disc together with the associated error bars recorded at the 95% level.

The crystallographic texture was measured on an area of 1×2 mm² by X-ray diffraction in a Siemens goniometer system. The X-ray radiation used was cobalt $K\alpha$ and seven $\{0002\}$, $\{11\bar{2}0\}$, $\{01\bar{1}1\}$, $\{01\bar{1}2\}$, $\{01\bar{1}3\}$, $\{11\bar{2}2\}$ and $\{02\bar{2}1\}$ incomplete pole figures were measured. The data were then analysed using the Arbitrarily Defined Cells (ADC) method with Labotex software to calculate the orientation distribution functions and the complete pole figures. The pole figures were recorded at the disc surface (r, θ) plane, perpendicular to the extrusion axis and torsion axis. The (r, θ) plane is the plane defined by the shear direction (SD: vertical axis) and the radial direction (RD: horizontal axis). Classically, the torsion texture orientations are labeled $\{hkil\}\langle uvtw \rangle$, where $\{hkil\}$ is a plane parallel to the shear plane and $\langle uvtw \rangle$ is a direction parallel to the shear direction.

3. Experimental Results

3.1. Microstructure and hardness development during HPT at 296 to 473 K

HPT processing of AZ31 was conducted easily at 296 and 373 K without introducing any cracking into the discs. Microstructural observations were taken at the disc centres, the half-radius positions and at the edge of each disc after HPT processing through 1 or 5 turns at temperatures of 296, 373 and 473 K. Figure 1 shows microstructures for the discs processed at the lowest temperature of 296 K after 1 turn. The microstructures after 1 turn showed that the centre and half-radius positions exhibit typical bi-modal grain size distributions with a relatively small fraction of coarser grains mixed with a large fraction of ultrafine grains. By contrast, the fractions and sizes of coarser grains were significantly reduced at the edge of the disc by comparison with the centre and half-radius positions. These results demonstrate that the grain structure tends to become more uniform from the centre to the edge along the radial direction, i.e. the microstructural evolution occurs more rapidly toward the peripheral region of the disc even when AZ31 is processed by HPT at room temperature. In Figure 1a, b, some twinning and segmented coarse grains exist in the disc centre and half-radius areas thereby indicating the twinning contribution to the deformation. The sample processed by HPT at 296 K through 5 turns had a similar variation in grain structure as the 1 turn sample. The microstructures of samples processed by HPT at 373 K were generally consistent with the microstructures attained at 296 K except for some differences in the measured grain sizes.

The average grain sizes and the associated error bars at the 95% level are shown in Table 1 for discs processed by 1 and 5 turns at the three different processing temperatures. These results provide valuable information on the trend for grain size evolution. It is apparent from Table 1 that the average grain size is reduced with increasing numbers of turns in HPT processing at 296 K. Thus, the average grain sizes at $N = 5$ tend to be finer than at $N = 1$ in the centre and at the half-radius, and also the edge values are smaller than the values at the half-radius and the centre. A similar grain size variation trend exists for the discs processed at 373 K and there is no evidence for grain growth at this temperature.

At the highest processing temperature of 473 K, there were no bi-modal grain size distributions either in the disc centre or near the edge. Observations after 1 turn showed

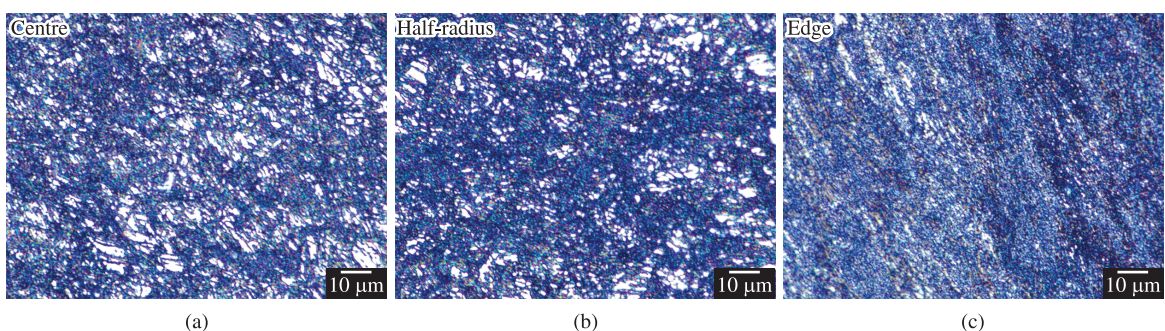


Figure 1. Microstructures after HPT processing at 296 K for $N = 1$ turn at (a) the centre, (b) the half-radius and (c) the edge of the disc.

the grain size distributions were more heterogeneous than at 296 and 373 K as coarser grains were present in the centre of the disc. Figure 2 shows the microstructures at 473 K after $N = 5$ turns. It is apparent that grain growth occurs at 473 K by comparison with the grain structures at the lower temperature of 296 K shown in Figure 1. The individual grain size measurements for the discs processed at 473 K are also shown in the lower section of Table 1. It is important to note that the measured grain sizes after $N = 5$ turns are now significantly larger, instead of smaller, than the grain sizes measured after $N = 1$ turn. These results demonstrate the occurrence of significant grain growth during processing from 1 to 5 turns at 473 K and this contrasts with the processing at 296 and 373 K where it is possible to achieve, and maintain with additional straining, a distribution of ultrafine grains. The grain growth process at 473 K becomes more significant when the processing time is increased. This is consistent with the necklace-like microstructure which is an inherent feature of

the dynamic recrystallization of magnesium alloys processed in the temperature range of ~ 400 – 600 K^[10,21,22]. In this process, new finer grains form along the original grain boundaries of the initial coarser structure and these finer grain gradually consume the larger grains and thereby produce an ultrafine structure. This refinement process for hcp metals is different from the grain refinement process for fcc metals under ECAP conditions where the large grains become subdivided by boundaries having low angles of misorientation²³ and these subgrain boundaries gradually evolve with increasing strain into high-angle boundaries^{24,25}.

The results of the Vickers microhardness distributions along the disc diameters are shown in Figure 3 for temperatures of (a) 296, (b) 373 and (c) 473 K, respectively. At 296 and 373 K, the hardness values show similar variations and the hardness after 5 turns is slightly above that after 1 turn as shown in Figure 3a, b. The hardness values are consistent with the corresponding microstructures at 296 K where the finer grain size at the disc centre and half-radius areas after 5 turns leads to higher hardness values than its counterpart processed by 1 turn and the similar ultrafine grain sizes at the disc edge after 1 and 5 turns lead to similar hardness values after 1 and 5 turns. At 373 K, the hardness level at the disc centre area shows almost no variation between 1 and 5 turns. A hardness drop in the centre areas is observed at 296 and 373 K compared to the edge of the disc after both 1 and 5 turns, thereby indicating an inhomogeneous microstructure. Due to grain growth at 473 K, with the longer processing time for 5 turns, the occurrence of grain growth leads to a lower hardness value after 5 turns in Figure 3c. The hardness along the disc diameters becomes more uniform at a temperature of 473 K for samples processed at both 1 and 5 turns.

Table 1. Results of average grain size and the associated error bars at different positions on the discs processed by 1 and 5 turns of HPT at 296, 373 and 473 K.

Temperature (K)	Number of turns	Position	Average grain size (mm)
296	1	Centre	1.4 ± 0.1
		Half-radius	1.2 ± 0.2
		Edge	0.9 ± 0.1
	5	Centre	1.2 ± 0.2
		Half-radius	1.0 ± 0.2
		Edge	0.9 ± 0.1
373	1	Centre	1.2 ± 0.4
		Half-radius	1.1 ± 0.2
		Edge	0.8 ± 0.2
	5	Centre	1.1 ± 0.1
		Half-radius	0.9 ± 0.2
		Edge	0.8 ± 0.1
473	1	Centre	2.4 ± 1.2
		Half-radius	1.2 ± 0.5
		Edge	1.0 ± 0.4
	5	Centre	4.2 ± 1.4
		Half-radius	2.6 ± 0.5
		Edge	2.3 ± 0.5

3.2. Texture development during HPT at 296 to 473 K

Figure 4 shows the $\{0001\}$ and $\{10\bar{1}0\}$ pole figures for the as-received AZ31. The results demonstrate that the initial texture is $\{hki0\}$ fibre which means $\{10\bar{1}0\}$ planes in the extruded condition lie perpendicular to the extrusion axis and the $\{0001\}$ planes generally lie parallel to the extrusion axis. Furthermore, it shows the hcp crystal c-axis is in the (r,θ) plane (also (RD, SD) plane) of the disc and therefore perpendicular to the HPT torsion axis. The development of this type fibre texture in extruded Mg alloys has been documented in other reports^{26–28}.

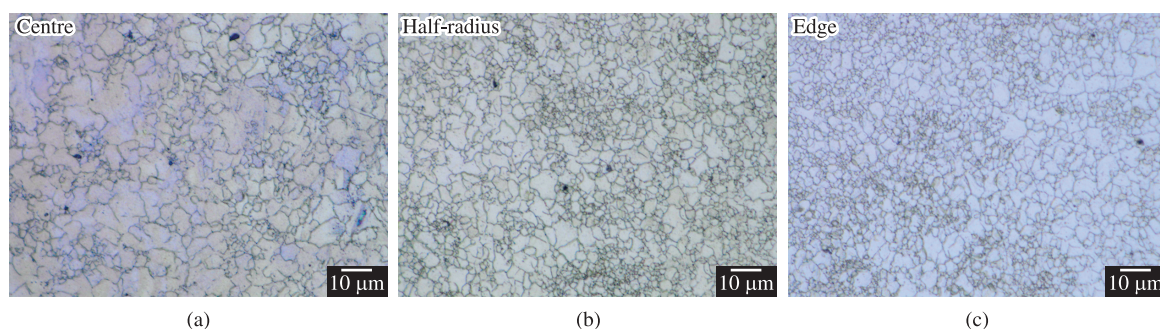


Figure 2. Microstructures after HPT processing at 473 K for $N = 5$ turns at (a) the centre, (b) the half-radius and (c) the edge of the disc.

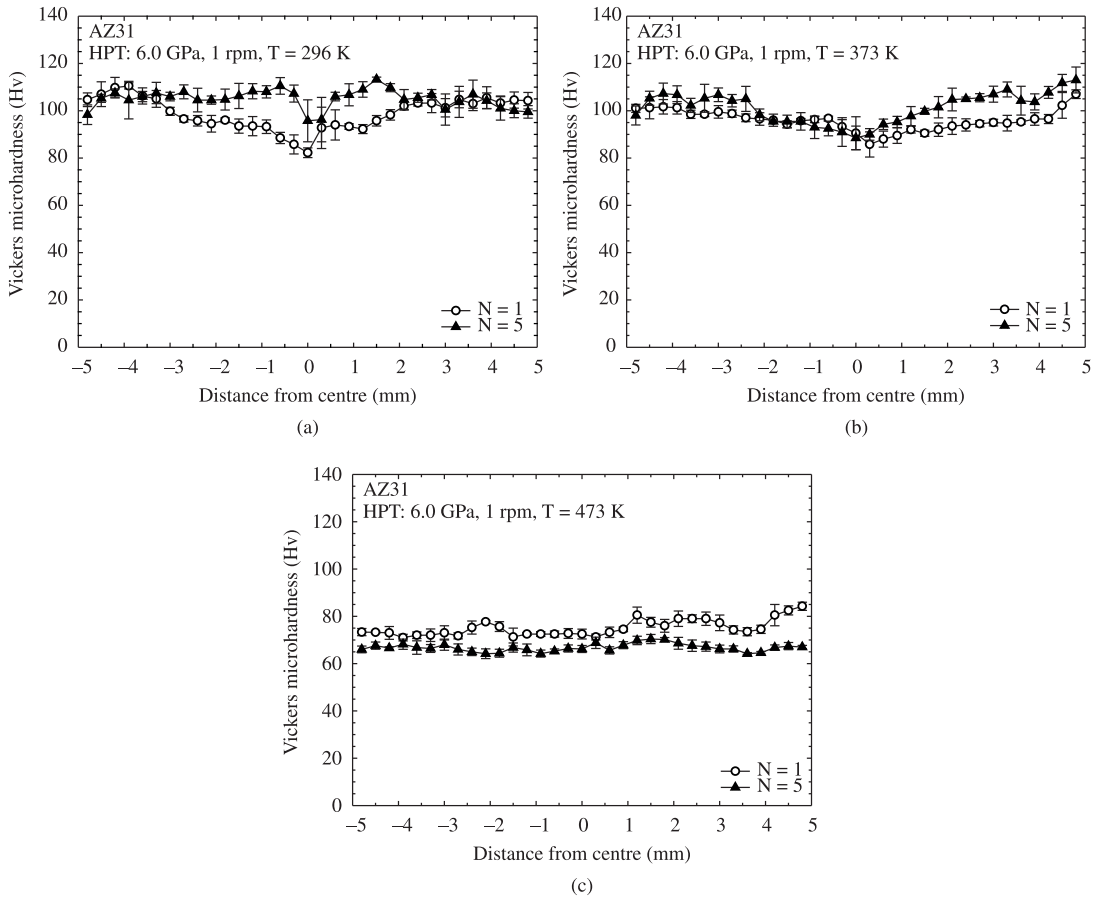


Figure 3. Vickers microhardness distributions along disc diameters in discs processed by HPT at temperatures of (a) 296 K, (b) 373 K and (c) 473 K.

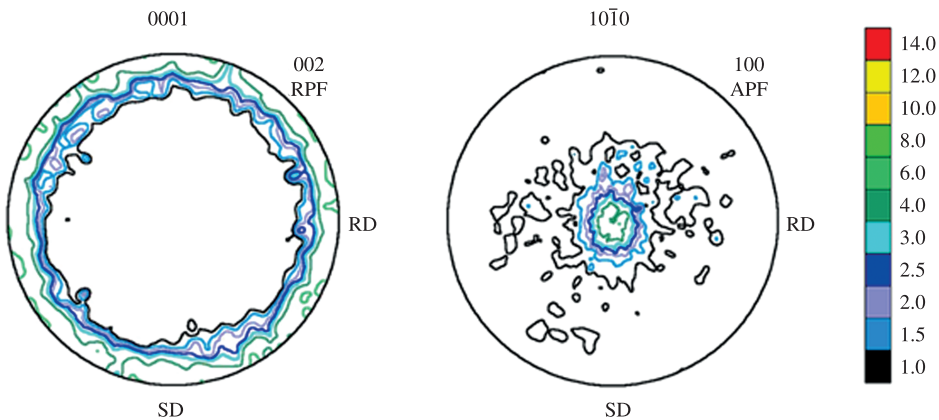


Figure 4. The $\{0001\}$ and $\{10\bar{1}0\}$ pole figures in the as-received AZ31 alloy.

Figures 5 and 6 show the texture variations with different HPT processing temperatures after 1 and 5 turns, respectively. After HPT processing at 473 K for $N = 1$ and $N = 5$ turns, the textures displayed in Figure 5c and Figure 6c are basically the same texture of $\{0001\}$ fiber but with a slightly different intensity. The $\{0001\}$ fiber intensity at 473 K increases from a max 15.6 at 1 turn

to a max 17.3 at 5 turns. Thus, a more steady-state texture appears at 5 turns. An $\{0001\}$ fiber means the hcp crystal c-axis is parallel to the HPT torsion axis at 473 K which is consistent with other results for torsion testing²⁹.

Figures 5a and 6a show that the textures after HPT processing at 296 K for $N = 1$ and $N = 5$ turns are in a transformation state from the as-received $\{hki\}$ fiber shown

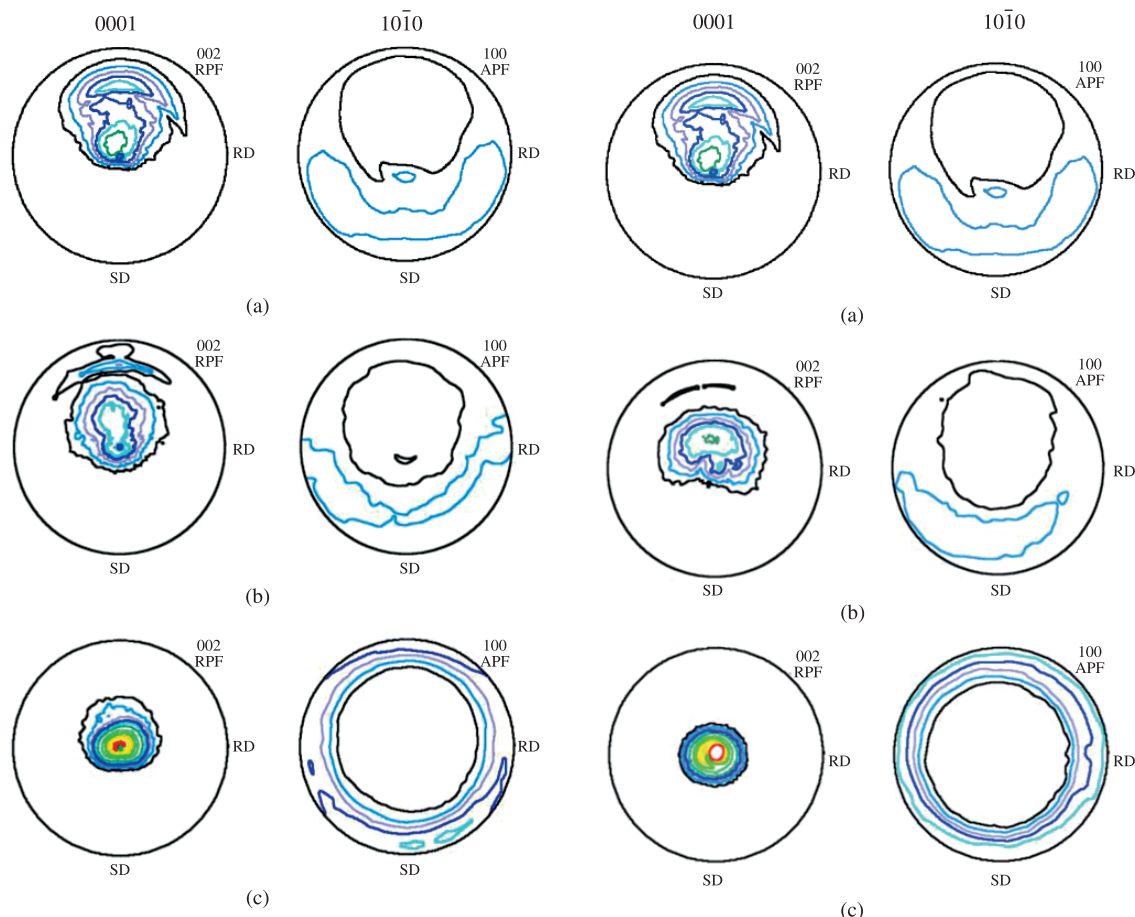


Figure 5. The $\{0001\}$ and $\{10\bar{1}0\}$ pole figures in discs processed by HPT with $N = 1$ turn at different temperatures: (a) 296 K, (b) 373 K and (c) 473 K.

Figure 6. The $\{0001\}$ and $\{10\bar{1}0\}$ pole figures in discs processed by HPT with $N = 5$ turns at different temperatures: (a) 296 K, (b) 373 K and (c) 473 K.

in Figure 4 to the $\{0001\}$ <uvw> fibre at 473 K shown in Figures 5c and 6c. At 296 K, the textures are made up of two components: the main $\{0001\}$ <uvw> fibre and a second fibre. After HPT processing at 373 K for $N = 1$ and $N = 5$ turns, the textures are also made up of two components: the main $\{0001\}$ <uvw> fibre and a second fibre, but the second fibre became weaker as the number of turns increases from 1 to 5. There is no significant difference in textures at 296 and 373 K with 1 and 5 turns and this similar texture at different temperatures is consistent with the earlier observations on microstructures and mechanical properties showing that at 296 and 373 K samples have similar grain sizes and hardness distributions during HPT processing.

The orientation distribution functions (ODF) of the as-received materials and the HPT processed samples are given in Figure 7. The ODF analysis shows that at 296 K in Figure 7b the texture is 10° rotated $\{0001\}$ <uvw> fibre (rotation around ϕ) + fibre1 ($\phi_1 = 87^\circ$, $\phi = 68^\circ$ and $\phi_2 = 0$ to 60°) for the 1 turn sample, and the texture is 10° rotated $\{0001\}$ <uvw> fibre (rotation around ϕ) + fibre2 ($\phi_1 = 146^\circ$, $\phi = 68^\circ$ and $\phi_2 = 0$ to 60°) for the 5 turns sample. During HPT processing at 296 K, the hcp c-axis of some grains rotate to a position which is more nearly parallel to the HPT torsion

axis but a second fibre remains in the other grains. At 373 K in Figure 7c, the texture is 10° rotated $\{0001\}$ <uvw> fibre (rotation around ϕ) + fibre1 ($\phi_1 = 87^\circ$, $\phi = 58^\circ$ and $\phi_2 = 0$ to 60°) for the 1 turn sample and the texture is 10° rotated $\{0001\}$ <uvw> fibre (rotation around ϕ) + fibre2 ($\phi_1 = 117^\circ$, $\phi = 58^\circ$ and $\phi_2 = 0$ to 60°) for the 5 turns sample. As the temperature is increased from 296 to 373 K, the second fibre gradually moves towards the torsion axis with the angle between the c-axis and the torsion axis (ϕ) decreasing from 68° to 58° . At 473 K in Figure 7d, the texture is 5° rotated $\{0001\}$ <uvw> fibre (rotation around ϕ) for both the 1 and 5 turns samples and the second fibres have disappeared. The intensity of texture at 473 K increases from max 18.9 of 1 turn to max 23.1 of 5 turns. The hcp crystal c-axis during HPT at 473 K is almost parallel to the HPT torsion axis without a second fibre.

4. Discussion

4.1. Influence of HPT temperature on microstructure

For both the $N = 1$ and $N = 5$ conditions, the material processed at 473 K has significantly coarser grains than

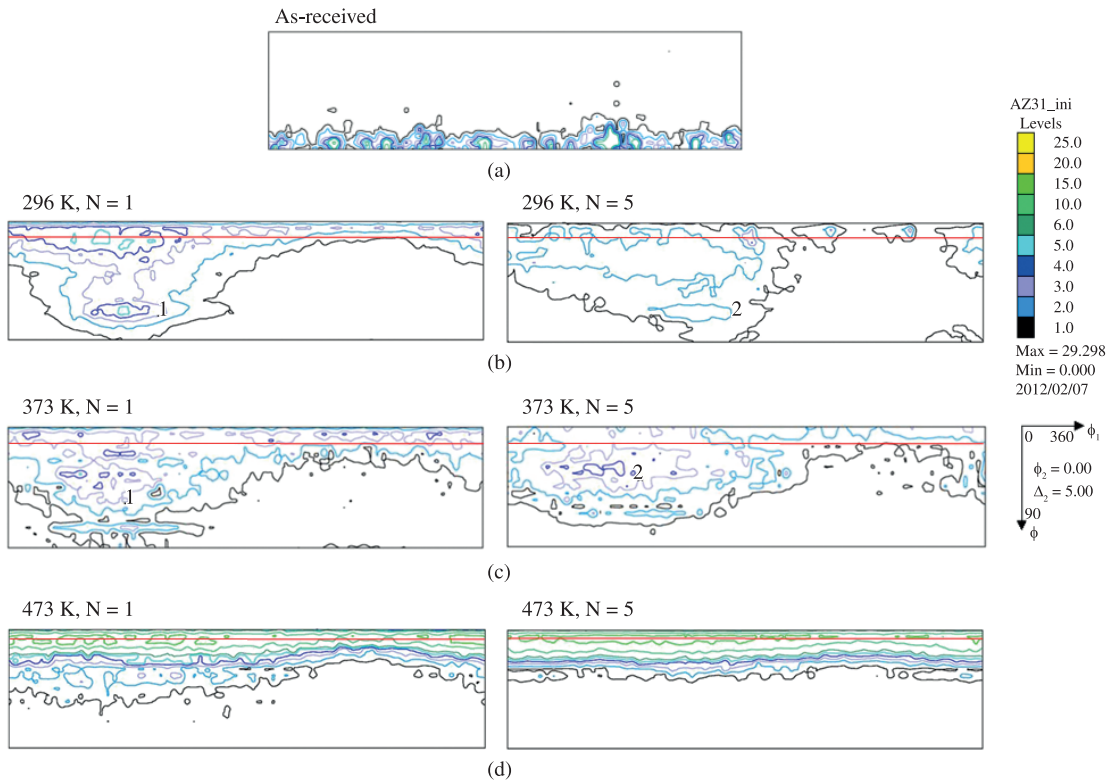


Figure 7. The orientation distribution function (ODF) of various HPT processing conditions: (a) as-received, (b) 296 K, $N = 1$ and $N = 5$ turns, (c) 373 K, $N = 1$ and $N = 5$ turns, (d) 473 K, $N = 1$ and $N = 5$ turns.

the materials processed at 373 and 296 K. At 296 K and 373 K, no grain growth occurs during HPT processing. The grain refinement appears to result from a fragmentation of the larger grains by twinning due to the severe shear deformation. At 473 K, grain refinement appears to result from two concurrent effects as suggested in an earlier report¹⁰: specifically, the formation of a large population of small recrystallized grains at the original grain boundaries and the fragmentation of the larger grains by twinning which serves as sites where new recrystallized grains are formed. Since the grain size is a major factor in determining the strength of the material, the maximum strength is achieved at the two lower temperatures of 296 and 373 K. These results therefore confirm the advantage of processing the AZ31 alloy at a relatively lower temperature. Thus, processing at 296 and 373 K avoids the problem of grain growth which is an inherent feature of processing at higher temperatures.

4.2. Influence of HPT temperature on texture

It has been reported that the critical resolved shear stress (CRSS) for basal plane slip in magnesium single crystals exhibits a 100 times lower value than for non-basal plane slip near room temperature³⁰. Consequently, the basal $\langle a \rangle$ slip systems $\{0001\}\langle 11\bar{2}0 \rangle$ are the easy glide systems in Mg. Although the prismatic $\langle a \rangle$ slip system $\{10\bar{1}0\}\langle 11\bar{2}0 \rangle$ and 1st-order pyramidal $\langle a \rangle$ slip system $\{10\bar{1}1\}\langle 11\bar{2}0 \rangle$ also operate in Mg, none of these systems is capable of accommodating strain along the c -axis direction. The activation of the 2nd-order pyramidal $\langle c+a \rangle$ slip system

$\{11\bar{2}2\}\langle 11\bar{2}3 \rangle$ is generally assumed to provide the required additional degree of freedom and it has a c -slip component but it depends strongly on temperature. Since deformation twinning in Mg is often easier than pyramidal $\langle c+a \rangle$ slip, twinning plays an important role to accommodate the deformation, particular at low temperatures. Two common twin modes have been observed in magnesium. These are classified as extension twins $\{10\bar{1}2\}\langle 10\bar{1}1 \rangle$ and contraction twins $\{10\bar{1}1\}\langle 10\bar{1}2 \rangle$ ^[31] because they result in an extension or contraction of the crystal along the c -axis direction, respectively. The extension twinning $\{10\bar{1}2\}$ is active in grains only when the deformation conditions are such that an extension along the c -axis takes place. When the c -axis of a Mg grain is placed under compression, the contraction twinning $\{10\bar{1}1\}$ may be activated.

Before HPT processing, the initial texture is $\{hk\bar{i}0\}$ fibre which means the hcp crystal c -axis is in the (r,θ) plane (also (RD, SD) plane) of the disc and perpendicular to the HPT torsion axis. The c -axis can be parallel to, perpendicular to, or having a certain angle to the torsion shear direction. When the c -axis is parallel to the shear direction, slip on the prismatic $\langle a \rangle$ or basal $\langle a \rangle$ planes is not possible because the Schmid factor is zero. When the c -axis is perpendicular to the shear direction, easy slip occurs on the prismatic planes. When the c -axis has a certain angle to the shear direction, it is possible for both prismatic $\langle a \rangle$ and pyramidal $\langle c+a \rangle$ slip to be activated. Considering the different possible orientations between the c -axis and the shear direction, basal

$\langle a \rangle$, prismatic $\langle a \rangle$, pyramidal $\langle c+a \rangle$ slip and deformation twinning may all make contributions to accommodate the torsion deformation in HPT processing.

It has been shown that the texture changes significantly with very low straining during compression if the direction of loading is perpendicular to the c -axis of the AZ31 alloy^{32,33}. This effect is attributed to twinning because when grains have their c -axis perpendicular to the compressive loading direction the extension twinning $\{10\bar{1}2\}$ becomes active. As a consequence, the c -axis of crystals is re-oriented nearly parallel to the loading direction: thus, a rotation of the c -axis by $\sim 90^\circ$ was observed at strains lower than 10% in compression. In fact, compression pressure along the axial direction of the disc is expected to take place prior to torsion straining in HPT because of the imposition of the applied pressure of 6.0 GPa. This compression direction is perpendicular to the c -axis of the as-received material and may lead to rotation and alignment of the c -axis towards the compression axial direction. This is in agreement with the observed variations in texture.

The effect of the HPT processing temperature on texture is shown in Figure 7. After HPT processing, the hcp crystal c -axis rotated from the disc (r,θ) plane (also (RD, SD) plane) towards the torsion axis. The angle between the c -axis and the torsion axis (ϕ) has a certain relationship with the HPT processing temperature. It was found that the c -axis of some grains was 10° from the torsion axis at 296 and 373 K but the c -axis of almost all grains was 5° from the torsion axis at 473 K.

At room temperature the deformation of Mg is strongly restricted to the basal $\langle a \rangle$ $\{0001\} \langle 11\bar{2}0 \rangle$ slip system and the extension twinning $\{10\bar{1}2\} \langle 10\bar{1}\bar{1} \rangle$ system³⁴. This limited number of available slip systems makes it difficult to successfully press Mg alloys by ECAP at room temperature. At the HPT processing temperatures of 296 and 373 K, some grains have their c -axis re-oriented almost 10° from the torsion axis under the compressive pressure but other grains have their c -axis tilted at angles more than 10° from the torsion axis. Grains that have their c -axis re-oriented almost 10° from the torsion axis will maintain their orientation with further shear deformation because the c -axis is almost perpendicular to the shear direction and this make basal slip $\langle a \rangle$ become the easiest process for accommodating shear deformation. For grains that have their c -axis tilted at angles more than 10° from the torsion axis, due to the limited slip systems available at lower temperatures, mainly basal slip $\langle a \rangle$ and deformation twinning may make contributions to accommodate the torsion deformation in HPT so that the orientation between the c -axis and the torsion axis will not change significantly. The twinning contribution is confirmed from the microstructures in Figures 2 and 8 in which twinning and segmented coarse grains are found in discs processed by HPT at 296 and 373 K.

By increasing the HPT processing temperature to 473 K, significant grain growth occurs and thermally-activated recovery processes are activated. The CRSS for non-basal slip decreases with increasing temperature and above 473 K the activation of dislocation motion in the pyramid $\langle c+a \rangle$ is energetically more favourable than twinning³⁵. Besides basal $\langle a \rangle$ slip and twinning, non-basal pyramid $\langle c+a \rangle$ slip system could be activated at high temperatures. This means the grains that are not fully aligned have more freedom to rotate towards an orientation where the c -axis is almost

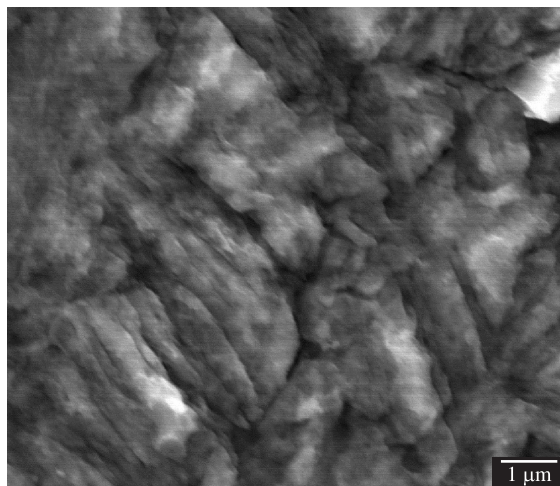


Figure 8. Microstructure after HPT processing at 373 K for $N = 1$ turn.

parallel to the torsion axis and thus to attain a stable texture state in which the basal $\langle a \rangle$ slip system accommodates the HPT shear deformation.

5. Summary and Conclusions

- Processing by HPT was conducted on an extruded AZ31 Mg alloy at 296, 373 and 473 K for 1 and 5 turns thereby confirming that HPT provides an opportunity for processing Mg alloys at lower temperatures than in conventional ECAP;
- Processing at 296 and 373 K leads to significant grain refinement whereas processing at 473 K is accompanied by grain growth during the processing operation. The hardness values at 473 K are smaller than at 296 and 373 K due to the occurrence of grain growth;
- The textures changes from the as-received $\{hki0\}$ fibre to the $\{0001\}$ fibre after HPT processing at 473 K so that the hcp crystal c -axis rotates from the disc (r,θ) plane towards the torsion axis. The angle between the c -axis and the torsion axis (ϕ) has a relationship with the HPT processing temperature. The results show the c -axis is 10° from the torsion axis at 296 and 373 K but 5° from the torsion axis at 473 K;
- The results demonstrate that the activity of the basal $\langle a \rangle$ slip and twinning exert significant contributions on the deformation.

Acknowledgements

Participation at NANOMAT-2012 was made possible through award FAPESP#2011/51245-8 under a cooperation agreement with the University of Southampton. This work was supported by the European Research Council under ERC Grant Agreement No. 267464-SPDMETALS. One of the authors (RBF) was supported by CNPq under Grant Agreement No. 483077/2011-9. The authors acknowledge D. Solas for assistance during the X-ray diffraction texture measurements.

References

1. Valiev RZ, Islamgaliev RK and Alexandrov IV. Bulk nanostructured materials from severe plastic deformation. *Progress in Materials Science*. 2000; 45:103-189. [http://dx.doi.org/10.1016/S0079-6425\(99\)00007-9](http://dx.doi.org/10.1016/S0079-6425(99)00007-9)
2. Valiev RZ and Langdon TG. Principles of equal-channel angular pressing as a processing tool for grain refinement. *Progress in Materials Science*. 2006; 51:881-981. <http://dx.doi.org/10.1016/j.pmatsci.2006.02.003>
3. Zhilyaev AP and Langdon TG. Using high-pressure torsion for metal processing: Fundamentals and applications. *Progress in Materials Science*. 2008; 53:893-979. <http://dx.doi.org/10.1016/j.pmatsci.2008.03.002>
4. Komura S, Horita Z, Nemoto M and Langdon TG. Influence of stacking fault energy on microstructural development in equal-channel angular pressing. *Journal of Materials Research*. 1999; 14:4044-4050. <http://dx.doi.org/10.1557/JMR.1999.0546>
5. Mishra A, Richard V, Gregori F, Asaro RJ and Meyers MA. Microstructural evolution in copper processed by severe plastic deformation. *Materials Science and Engineering A*. 2005; 410-411:290-298. <http://dx.doi.org/10.1016/j.msea.2005.08.201>
6. Iwahashi Y, Horita Z, Nemoto M and Langdon TG. The process of grain refinement in equal-channel angular pressing. *Acta Materialia*. 1998; 46:3317-3331. [http://dx.doi.org/10.1016/S1359-6454\(97\)00494-1](http://dx.doi.org/10.1016/S1359-6454(97)00494-1)
7. Xu C, Furukawa M, Horita Z and Langdon TG. The evolution of homogeneity and grain refinement during equal-channel angular pressing: A model for grain refinement in ECAP. *Materials Science and Engineering A*. 2005; 398:66-76. <http://dx.doi.org/10.1016/j.msea.2005.03.083>
8. Eddahabi M, del Valle JA, Perez-Prado MT and Ruano OA. Comparison of the microstructure and thermal stability of an AZ31 alloy processed by ECAP and large strain hot rolling. *Materials Science and Engineering A*. 2005; 410-411:308-311. <http://dx.doi.org/10.1016/j.msea.2005.08.081>
9. Lapovok R, Estrin Y, Popov MV, Rundell S and Williams T. Enhanced superplasticity of magnesium alloy AZ31 obtained through equal-channel angular pressing with back-pressure. *Journal of Materials Science*. 2008; 43:7372-7378. <http://dx.doi.org/10.1007/s10853-008-2685-z>
10. Figueiredo RB and Langdon TG. Grain refinement and mechanical behaviour of a magnesium alloy processed by ECAP. *Journal of Materials Science*. 2010; 45:4827-4836. <http://dx.doi.org/10.1007/s10853-010-4589-y>
11. Figueiredo RB, Cetlin PR and Langdon TG. The processing of difficult-to-work alloys by ECAP with an emphasis on magnesium alloys. *Acta Materialia*. 2007; 55:4769-4779. <http://dx.doi.org/10.1016/j.actamat.2007.04.043>
12. Kang F, Wang JT and Peng Y. Deformation and fracture during equal channel angular pressing of AZ31 magnesium alloy. *Materials Science and Engineering A*. 2008; 487:68-73. <http://dx.doi.org/10.1016/j.msea.2007.09.063>
13. Figueiredo RB, Cetlin PR and Langdon TG. Stable and unstable flow in materials processed by equal-channel angular pressing with an emphasis on magnesium alloys. *Metallurgical and Materials Transactions A*. 2010; 41A:778-786.
14. Cetlin PR, Aguilar MTP, Figueiredo RB and Langdon TG. Avoiding cracks and inhomogeneities in billets processed by ECAP. *Journal of Materials Science*. 2010; 45:4561-4570. <http://dx.doi.org/10.1007/s10853-010-4384-9>
15. Serre P, Figueiredo RB, Gao N and Langdon TG. Influence of strain rate on the characteristics of a magnesium alloy processed by high-pressure torsion. *Materials Science and Engineering A*. 2011; 528:3601-3608. <http://dx.doi.org/10.1016/j.msea.2011.01.066>
16. Figueiredo RB and Langdon TG. Development of structural heterogeneities in a magnesium alloy processed by high-pressure torsion. *Materials Science and Engineering A*. 2011; 528:4500-4506. <http://dx.doi.org/10.1016/j.msea.2011.02.048>
17. Figueiredo RB and Langdon TG. Structural evolution on the cross-section of an AZ31 magnesium alloy processed by high-pressure torsion. *Materials Science Forum*. 2011; 667-669:247-252. <http://dx.doi.org/10.4028/www.scientific.net/MSF.667-669.247>
18. Huang Y, Figueiredo RB, Baudin T, Helbert A-L, Brisset F and Langdon TG. Effect of temperature on the processing of a magnesium alloy by high-pressure torsion. *Journal of Materials Science*. 2012; 47:7796-7806. <http://dx.doi.org/10.1007/s10853-012-6578-9>
19. Huang Y, Figueiredo RB, Baudin T, Brisset F and Langdon TG. Evolution of strength and homogeneity in a magnesium AZ31 alloy processed by high-pressure torsion at different temperatures. *Advanced Engineering Materials*. 2012; 14(11):1018-1026. <http://dx.doi.org/10.1002/adem.201200016>
20. Harai Y, Kai M, Kaneko K, Horita Z and Langdon TG. Microstructural and mechanical characteristics of AZ61 magnesium alloy processed by high-pressure torsion. *Materials Transactions*. 2008; 49:76-83. <http://dx.doi.org/10.2320/matertrans.ME200718>
21. Figueiredo RB and Langdon TG. Principles of grain refinement in magnesium alloys processed by equal-channel angular pressing. *Journal of Materials Science*. 2009; 44:4758-4762. <http://dx.doi.org/10.1007/s10853-009-3725-z>
22. Figueiredo RB and Langdon TG. The nature of grain refinement in equal-channel angular processing: a comparison of representative fcc and hcp metals. *International Journal of Materials Research*. 2009; 100:1638-1646. <http://dx.doi.org/10.3139/146.110228>
23. Langdon TG. The principles of grain refinement in equal-channel angular pressing. *Materials Science and Engineering A*. 2007; 462:3-11. <http://dx.doi.org/10.1016/j.msea.2006.02.473>
24. Kawasaki M, Horita Z and Langdon TG. Microstructural evolution in high purity aluminium processed by ECAP. *Materials Science and Engineering A*. 2009; 524:143150. <http://dx.doi.org/10.1016/j.msea.2009.06.032>
25. Xu C, Horita Z and Langdon TG. Microstructural evolution in an aluminium solid solution alloy processed by ECAP. *Materials Science and Engineering A*. 2011; 528:6059-6065. <http://dx.doi.org/10.1016/j.msea.2011.04.017>
26. Mukai T, Yamanoi M, Watanabe H and Higashi K. Ductility enhancement in AZ31 magnesium alloy by controlling its grain structure. *Scripta Materialia*. 2001; 45:89-94. [http://dx.doi.org/10.1016/S1359-6462\(01\)00996-4](http://dx.doi.org/10.1016/S1359-6462(01)00996-4)
27. Lin HK, Huang JC and Langdon TG. Relationship between texture and low temperature superplasticity in an extruded AZ31 Mg alloy processed by ECAP. *Materials Science and Engineering A*. 2005; 402:250-257. <http://dx.doi.org/10.1016/j.msea.2005.04.018>
28. Estrin Y, Yi SB, Brokmeier H-G, Zúberová Z, Yoon SC, Kim HS et al. Microstructure, texture and mechanical properties of the magnesium alloy AZ31 processed by ECAP. *International*

- Journal of Materials Research*. 2008; 99:50-55. <http://dx.doi.org/10.3139/146.101611>
29. Beausir B, Tóth LS and Neale KW. Ideal orientation and persistence characteristics of hexagonal close packed crystals in simple shear. *Acta Materialia*. 2007; 55:2695-2705. <http://dx.doi.org/10.1016/j.actamat.2006.12.021>
30. Reed-Hill RE and Robertson WD. Deformation of magnesium single crystal by non-basal slip. *Journal of Metal*. 1957; 9:496-502.
31. Wang YN and Huang JC. Texture analysis in hexagonal materials. *Materials Chemistry and Physics*. 2003; 81:11-26. [http://dx.doi.org/10.1016/S0254-0584\(03\)00168-8](http://dx.doi.org/10.1016/S0254-0584(03)00168-8)
32. Yi SB, Davies CHJ, Brokmeier HG, Bolmaro RE, Kainer KU and Homeyer J. Deformation and Texture evolution in AZ31 magnesium alloy during uniaxial loading. *Acta Materialia*. 2006; 54:549-562. <http://dx.doi.org/10.1016/j.actamat.2005.09.024>
33. Dudamell NV, Ulacia I, Gálvez F, Yi S, Bohlen J, Letzig D et al. Twinning and grain subdivision during dynamic deformation of a Mg AZ31 sheet alloy at room temperature. *Acta Materialia*. 2011; 59:6949-6962. <http://dx.doi.org/10.1016/j.actamat.2011.07.047>
34. Leiva DR, Fruchart D, Bacia M, Girad G, Skryabina N, Villela ACS et al. Mg alloy for hydrogen storage processed by SPD. *International Journal of Materials Research*. 2009; 100:1739-1746. <http://dx.doi.org/10.3139/146.110225>
35. Máthys K, Nyilas K, Axt A, Dragomir-Cernatescu I, Ungár T and Lukáč P. The evolution of non-basal dislocations as a function of deformation temperature in pure magnesium determined by x-ray diffraction. *Acta Materialia*. 2004; 52:2889-2894. <http://dx.doi.org/10.1016/j.actamat.2004.02.034>